

EXPERIMENTAL STUDY OF THE ACOUSTIC-COHERENT STRUCTURE COUPLING ON A SIMPLIFIED GEOMETRY INSTALLATION

S. PAUZIN, D. BIRON and P. HEBRARD

ONERA/CERT/DERMES
2, Avenue Edouard Belin, 31055 Toulouse Cedex
FRANCE

ABSTRACT

In order to study the acoustic-coherent structures coupling, a simplified geometry installation, in which a prismatic bluff body is placed, has been developed and tested. A coupling has been put forward when the vortex shedding and acoustic mode frequencies are close. The shift of the vortex shedding has been also investigated.

INTRODUCTION

In many cases, acoustic processes play a determining role in combustion instabilities. The existence of eigenmodes of the combustion cavity is often related to appearance of unstable combustion. The interaction of vortex shedding mechanism with combustion has been put in evidence, for example, by SMITH et al (1985) and POINSOT et al (1987). The coupling of acoustics with coherent structure is also important in cold flow. Various experimental arrangements of the flow around bluff bodies have been examined. HUSSAIN et al (1976) observe an amplitude modulation of the vortex street signal in a flow (low Reynolds number) superimposed with sound, OKAMOTO et al (1981) find an influence of sound radiated into the flow parallel to a cylinder on vorticity, shedding frequency and correlation along the span of the cylinder. The effect of transverse standing acoustic waves is investigated by BLEVINS (1985). He finds a shift of the vortex shedding toward the sound frequency. This paper deals with an experimental study carried out on a simplified installation in cold flow. A flameholder is simulated and the existence of a threshold versus acoustic level and discrepancy in frequency is investigated.

The wake structure of the vortex shedding is also examined.

DESCRIPTION OF EXPERIMENTAL APPARATUS AND INSTRUMENTATION

The apparatus used for our experiment is illustrated in fig. 1. Atmospheric air flows through an entrance into a duct of $15 \times 10 \text{ cm}^2$ rectangular cross section, in which a prismatic bluff body is placed in cross flow. It consists of a 3 cm side square rod. The exit section is constituted by a variable throat sonic nozzle. The length of the test duct is $L = 1.85 \text{ m}$. Two loudspeakers in enclosure are shunt connected close to the air entrance to provide acoustical excitation. A maximum of 145 db (ref. $2 \times 10^5 \text{ Pa}$) of sound pressure level is superimposed upon the flow field to investigate interferences in vortex shedding from the prismatic body. The mean velocity value of the flow is $v = 9 \text{ m/s}$ and the Reynolds number ($Re = Ud/v$) tested is 2.5×10^4 (d , diagonal of the square rod). Mean and fluctuating velocity profiles are performed, upstream of the square rod, with a hot wire

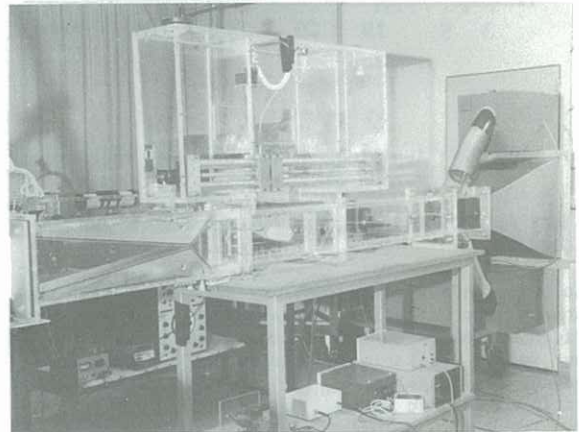


Fig. 1 : View of the installation

anemometer mounted on a movable support. The acoustic sensors consist of two B&K (1/8 in) condenser microphones fitted with nose cone and mounted on a movable probe. The microphones are located near the two symmetrical vortex streets. The signals are stored on a tape recorder or on a microcomputer IBM XT connected with a two channel analyzer (2032 B&K). Each measurement spectrum is obtained after an average of 1000 consecutive spectra. The frequency resolution is 2 Hz except when the zoom function is used (increasing resolution). The spectra are plotted with a linear frequency scale. Flow visualization is also performed using smoke. The KODAK EKTAPRO 1000 motion analyzer is used to permit recording up to 6000 images/s.

AERODYNAMIC AND ACOUSTIC INVESTIGATIONS

Horizontal and vertical velocity distributions are measured. The results show smooth profiles at the bluff body location in the test section ($0.2 < r/R < 0.8$) and low turbulence levels ($< 0.05\%$) in the same region. Then, the modal distribution and the characterization of the propagation in the duct are carried out. The first longitudinal mode is found at $f_a = 46 \text{ Hz}$ ($f_a = C/4L$, $C = 340 \text{ m/s}$) which is in agreement with the theoretical value. The values of the first transversal modes are, respectively, 1100 Hz for the height and 1711 Hz for the width. An investigation between different sections shows that the propagation is a plane wave field. The natural frequency and amplitude of the vortex shedding signal are also determined. A single well defined peak at the vortex shedding frequency is obtained. The Strouhal number is approximately 0.23 in the previous Reynolds number range. This value is in good agreement with result found in literature : IGARASHI (1984). The evolution of the magnitude of the vortex signal versus mean velocity

is the following one (fig. 2) :

$$A \text{ (Pa)} \sim 0.87 \times V^{1.65} \text{ (m/s)}$$

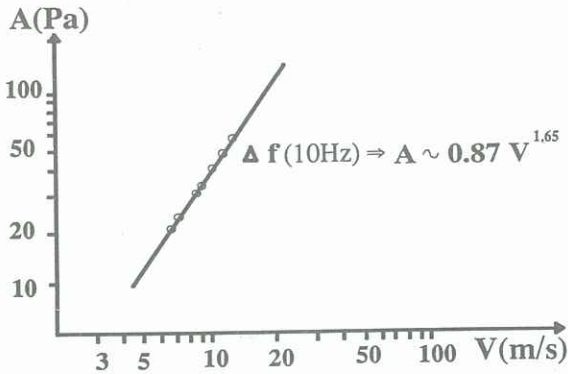


Fig. 2 : Amplitude of the Strouhal frequency versus mean velocity.

STUDY OF COUPLING BETWEEN VORTEX SHEDDING AND ACOUSTIC

In order to study the coupling between the two phenomena, the acoustical frequency ($f_a = 46 \text{ Hz}$), provided by the first longitudinal mode (with or without forced excitation), fits in the Strouhal frequency ($f_{st} = 46 \text{ Hz}$, $V = 8.6 \text{ m/s}$). An amplification ratio is defined as :

$$R = A_r^2 / (A_j^2 + A_e^2 - A_b^2)$$

The different amplitudes correspond to the configurations described on the scheme fig. 3. Each of them is analyzed on a band width of $\Delta F = 10 \text{ Hz}$ centered on the Strouhal frequency.

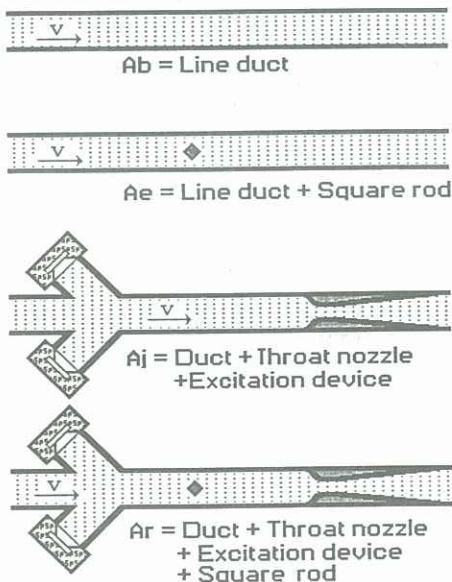


Fig. 3 : Sketch of configurations.

In the case of superimposition of the natural mode alone, one cannot observe any amplification. This is due to the fact that the level of the first longitudinal mode is very low facing to the level of the shedding signal (minus 10^2 , $\Delta = 40 \text{ db}$, $R \sim 1$ (PAUZIN et al 1988). When a forced excitation is applied at different levels (80 - 146 db), f_a locks in on the shedding frequency f_{st} , the curve of fig. 4 is obtained.

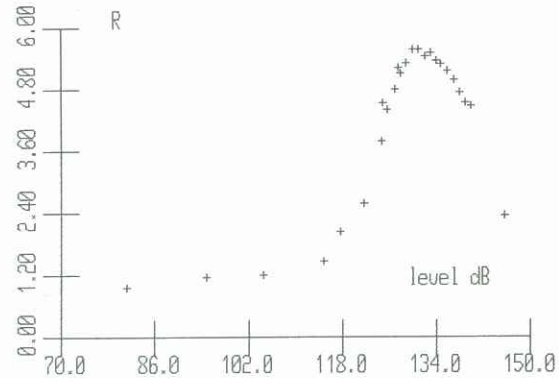


Fig. 4 : Amplification ratio vs excitation level.

The same investigation is made for a constant level of excitation (129 db, 46 Hz), the mean flow velocity varying (7 - 13 m/s), in order to see the effect of shift in frequency ($f_a \neq f_{st}$). The results are drawn on fig. 5.

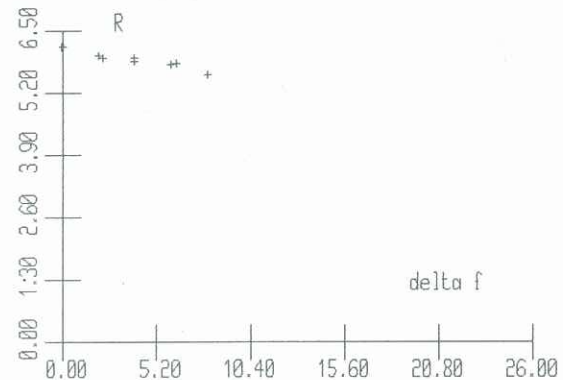


Fig. 5 : Amplification ratio vs $|f_a - f_{st}|$

Some considerations may be done about these results: an important amplification is put forward when the acoustical frequency is superimposed and matched sufficiently closely to the vortex shedding one. We find out the maximum of the curve ($R = 6$, fig. 4) for excitation levels are large as 130 db. These values correspond to a level of 10db above the magnitude of the vortex signal without acoustic. Then, increasing the excitation level involves $A_e \ll A_j$, so, $R \rightarrow A_j^2 / A_j^2 \rightarrow 1$. These results are in very good agreement with those published by PETERKA et al (1969) for same levels of excitation (135 - 140 db). Fig. 5 shows up that, when the two frequencies are not close together ($f_a \neq f_{st}$), there is still a significant amplification ratio ($f_{st} = 1.56 f_a$, $R = 4$). Then, the shift of the vortex shedding frequency is investigated. Like BLEVINS (1985), we point out that greater shift can be obtained for frequencies below the frequency occurring naturally than for frequencies above it. In the two works, the particle velocity is of the same order (2 - 3 % of the mean

velocity). Our research shows that, when the sound amplitude is sufficiently high (140 db) and the acoustic frequency close to the Strouhal frequency, the natural vortex shedding peak is suppressed and the peak at the acoustic frequency increases (fig. 6, PAUZIN et al (1988)).

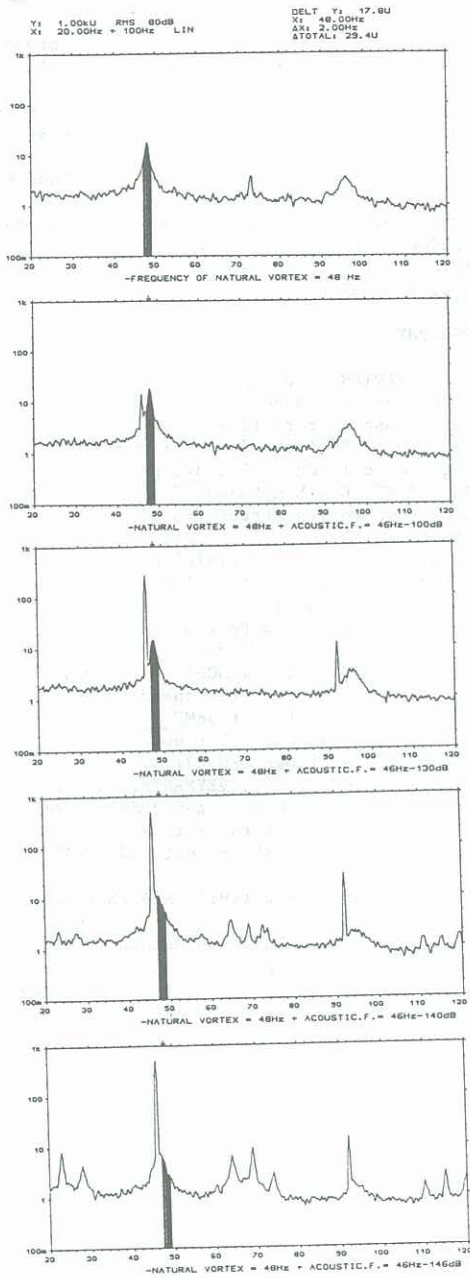


Fig. 6 : shift of f_{st} vs excitation.

These results are analyzed with the zoom function (20 - 120 Hz), the resolution is 0.15 Hz and the power in each case is measured with a bandwidth of 2 Hz centered on the frequency of interest. Table 1 shows the effects of acoustic level and frequency gap on the disappearing of the Strouhal frequency.

F_a frequency of the acoustic excitation
 $\Delta F = F_{st} - F_a$ gap between the two frequencies
 F_{st} vortex shedding frequency
 ΔF_{st} = difference in frequency level with and without excitation.

ΔF (Hz)	F_a level (db)	ΔF_{st} level (db)
2	110	0
	120	-0.1
	130	-0.9
	140	-4.3
	145.8	-8.6
4	120	-0.7
	130	-1.4
	140	-5.0
	145.5	-7.1
6	145.8	-6.3

one can observe that, when the gap between f_{st} and f_a increases, the effect on the shifting decreases even high frequency level. Applied sound centres the vortex shedding frequency at the frequency of excitation. Then, phase measurements have been achieved. The transfer function between the signals supplied by the two microphones located near the vortex streets is carried out. The phase value between the two vortex streets, without excitation, is approximately 180 degrees in the 42 - 52 Hz frequency range (cf. fig. 7.a). There is no phase relationship in other frequency range. The value of the coherence function is 1 around the Strouhal frequency (bandwidth of $\Delta F = 6$ Hz). These results are in good agreement with the wake structure of the flow behind this kind of obstacle. For low amplification ratio ($R < 1.4$) and for the frequency of excitation at the spectrum line, the phase decreases slightly and the value of the coherence function decreases rapidly (ex : $R = 1.22$, coherence = 0, cf. fig. 7b)

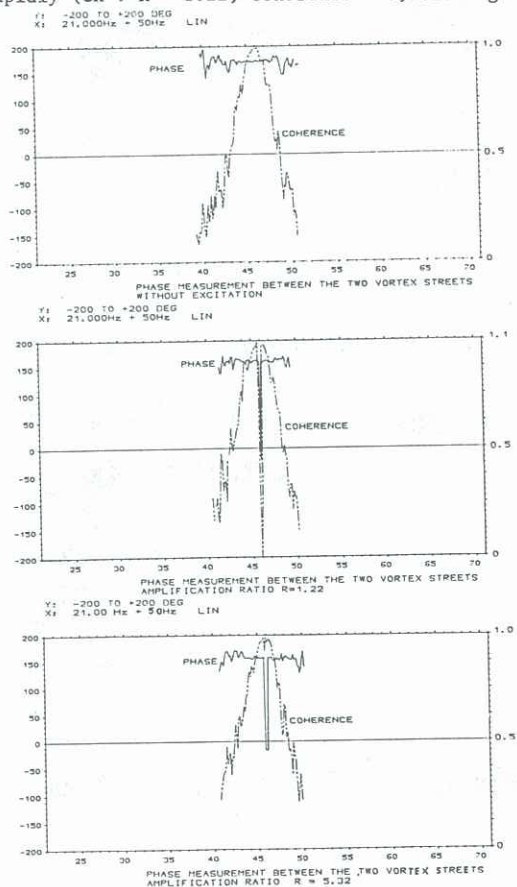


Fig. 7 : Phase measurement versus frequency at different excitation levels.

For high amplification ratio ($R > 2$), for the previous frequency, the phase value decreases rapidly ($\rightarrow 0$) and the coherence becomes again equal to 1 (cf. fig. 7c). One can see that, only, the phase at the excitation frequency is modified. The phase remains ~ 180 degrees around the Strouhal frequency whatever the acoustic level may be.

VISUALIZATIONS

A smoke machine is located at the air entrance and produces dense white smoke. The fluid is water based with a mixing of glycol and small particles of average size of 1 - 5 microns. Different techniques of lighting have been tried. Shadowgraphy is the best one. Two spotlights of 1000 W are used to obtain a $15 \times 20 \text{ cm}^2$ diffuse light field. Recordings are performed at 1000 images/s.

Qualitative comments may be done :

Without excitation, alternate vortex shedding appears in the near wake, in accordance with phase measurements (cf. fig. 8a). The vortices are rapidly diffused and convected with downstream flow. With sound superimposed at $f_a = f_{st}$, the vortex street geometry is modified as function of acoustic power level. When the amplitude of f_a ($< 110 \text{ dB}$) is low compared to vortex signal, the vortex street is similar to the previous one. This result agrees well with those of BARBI et al (1986), STRZELECKI (1989). For acoustic power level of 130 dB (R_{max}), it seems that vortex streets are more coherent than previously. The length of the formation region seems to increase (cf. Fig. 8b). At higher sound level ($> 140 \text{ dB}$), each vortex has minus time to develop and one can observe periodic smoke pulses but no vortices. Because of the small percentage of acoustic velocity value with regard

to mean velocity value and of the Reynolds number range, one cannot notice different variety of wake structures like DETEMPLELAAKE (1989). Further experiments have to be carried out in this domain.

CONCLUSION

An amplification phenomenon has been put forward when acoustic and Strouhal frequencies are close and when acoustic level is 10 dB above the vortex signal magnitude. Shift in frequency occurs when the sound frequency is close and below the Strouhal frequency. Further visualizations have to be carried out with an appropriate image processing to better understand of the phenomenology of the vortex streets with sound superimposed. This research is included in a complete study of combustion instabilities at the ONERA Center. A theoretical approach will be also lead.

BIBLIOGRAPHY

- BARBI, C., FAVIER, D.P., MARESCA, C.A., TELIONIS, D.P. (1986) vortex shedding and lock on a circular cylinder in oscillatory flow. *JFM*, 170, pp 527-544
- BLEVINS, R.D. (1985) the effect of sound on vortex shedding from cylinders *JFM*, 37, pp 217-237
- DETEMPLE-LAAKE, E., ECKELMANN, H. (1989) phenomenology of Karman vortex streets in oscillatory flow, *Experiments in fluids*, 7, pp 217-227
- HUSSAIN, A.K., RAMJEE, V. (1976) periodic wake behind a circular cylinder at low Reynolds number *AERONAUT Q* 27 pp 123-142
- IGARASHI, T (1984) characteristics of the flow around a square prism. *Bulletin of JSME*, 27, n° 231
- OKAMOTO, S., HIROSE, T., ADACHI, T. (1981) the effect of sound on the vortex shedding from a circular cylinder. *Bulletin of JSME* 24, 187
- PETERKA, J.A RICHARDSON, P.D (1969) effects of sound on separated flows *JFM*, 37 pp 265
- POINSOT, T.J, TROUVE, A.C, VEYNANTE, D.P, CANDEL, S.M, ESPOSITO, E.J (1987) vortex driven acoustically coupled combustion instabilities *JFM* 177, 265
- PAUZIN, S. BIRON, D (1988) report 1.2298/MES and report 1.2336/MES
- SMITH, D.A. ZUKOSKI, E.E (1985) AIAA/SAE/ASME 21 st joint prop conf
- STRZELECKI, A. (1989) Etude du détachement tourbillonnaire en écoulement perturbé : application à la débitmétrie vortex, University thesis, Toulouse.

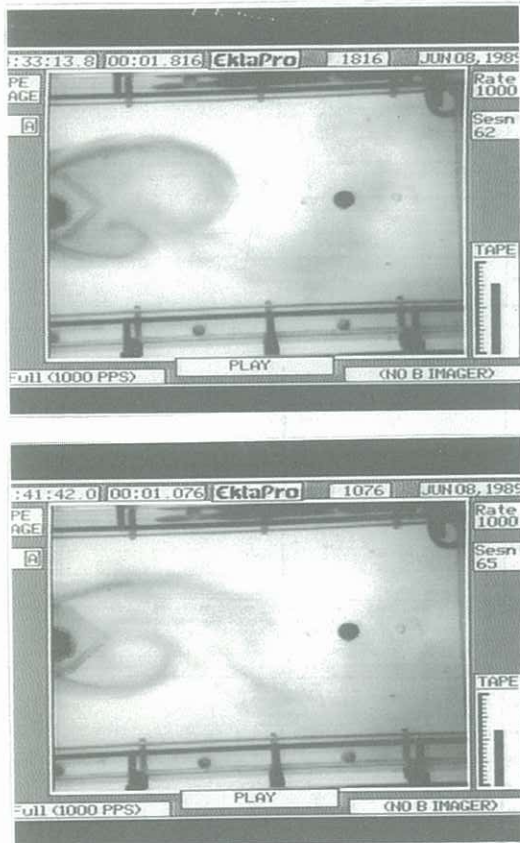


Fig. 8 : Flow visualizations with and without sound